29th International Cosmic Ray Conference Pune (2005) **6**, 85–88

Observation of the Anisotropy of 10 TeV Primary Cosmic Ray Nuclei Flux with the Super-Kamiokande-I Detector

G. Guillian[a] for the Super-Kamiokande Collaboration
(a) University of Hawaii, Manoa, 2505 Correa Rd., Honolulu, HI, 96822, USA
Presenter: G. Guillian (guillian@phys.hawaii.edu), usa-guillian-G-abs1-he11-oral

The relative sidereal variation in the arrival direction of primary cosmic ray nuclei of median energy 10 TeV was measured using downward, through-going muons detected with the Super-Kamiokande-I detector. The anisotropy map projected onto the right ascension axis has a first harmonic amplitude and phase of $(6.64 \pm 0.98 \text{ stat.} \pm 0.55 \text{ syst.}) \times 10^{-4}$ and $(33.2^\circ \pm 8.2^\circ \text{ stat.} \pm 5.1^\circ \text{ syst.})$, respectively. A sky map in equatorial coordinates indicates an excess (deficit) region in the constellation of Taurus (Virgo). The excess region is centered at $(\alpha_T, \delta_T) = (75^\circ \pm 7^\circ, -5^\circ \pm 9^\circ)$ with half opening angle $\chi_T = (39 \pm 7)^\circ$; the excess flux is $(0.104 \pm 0.020)\%$ above the isotropic expectation. The corresponding parameters for the deficit region are: $(\alpha_V, \delta_V) = (205^\circ \pm 7^\circ, 5^\circ \pm 10^\circ)$, $\chi_V = (54 \pm 7)^\circ$, and $(-0.094 \pm 0.014)\%$.

1. Introduction

Primary cosmic rays with energy per nucleon in the range $10^{11} \sim 10^{14}$ eV are known to have small but significant sidereal anisotropy of about several times 10^{-4}. The anisotropy is due to a combination of effects. Compton and Getting [1] proposed in 1935 that the motion of the solar system relative to the rest frame of the cosmic ray plasma should cause an energy independent dipole anisotropy with maximum in the direction of motion. Solar diurnal and seasonal changes in the atmospheric temperature can induce sidereal variation in the cosmic ray rate [2]. The anisotropy that remains after accounting for these effects is presumably of Galactic origin, with possible modulations due to the heliosphere (see, for example, [3, 4]) and, at the lowest energies, solar wind and magnetic field.

In this article, we report on the observation of cosmic ray anisotropy with the Super-Kamiokande I (SK-I) detector. SK-I is able to make a unique contribution to this subject because of the large overburden depth and detector size. The overburden causes SK-I to be sensitive to primary cosmic ray energies normally attainable with extensive air shower arrays. The large statistics and excellent muon tracking resolution enabled us to create a 2-dimensional mapping of the anisotropy, which is the first published muon-based map [1].

2. The Detector and the Data

SK-I is a 50 kiloton underground imaging water Cherenkov detector in Kamioka, Japan at geographical coordinates $36^\circ 25' 32.6'' \text{ N}$, $137^\circ 18' 37.1'' \text{ E}$ and an altitude of 370 m above sea level. The muon threshold energy is $\approx$ 1 TeV, which corresponds to a median primary cosmic ray energy of $\approx$ 10 TeV [6]. The detector area is between 1000 m^2 and 1200 m^2 depending on the zenith angle. The average event rate was 1.8 Hz. More details about the SK-I detector are reported in [7].

The data used in this analysis were collected between June 1, 1996 and May 31, 2001. A total of 2.54×10^8 muon events were collected in this period, with total detector live time of 1662.0 days, corresponding to a 91.0% live time fraction. Muon track reconstruction was performed with the standard algorithm developed

[1] Such a map was made using data from the IMB experiment and was reported in Gary McGrath's Ph. D. thesis [5], but the statistical significance was marginal and it was not published. The anisotropy reported there is qualitatively similar to our observations.

in SK-I to examine the spatial correlation between spallation products and parent muons in the solar neutrino analysis [8]. In order to maintain the angular resolution within 2°, the muons were required to have a track length greater than 10 m and be downward-going. The total number of muon events after these cuts is 2.10×10^8, corresponding to an efficiency of 82.6%.

The overburden at Kamioka causes the detector to be exposed unequally to the celestial sphere. The unevenness is mostly removed by exposing the sky over many revolutions of the earth. After five years, the residual unevenness in exposure was $^{+1.4\%}_{-1.3\%}$. In the celestial coordinate analysis of Sec. 3, the exposure was equalized by measuring the detector live time as a function of local sidereal time and applying a positive weight for events that occurred when the local sidereal time corresponded to the part of the sky that received below-average exposure, and vice versa for directions with above-average exposure.

The atmosphere is a part of the detector in the sense that it is responsible for converting primary cosmic rays into muons that can penetrate the overburden. It is a dynamic detector component because its density changes with temperature and pressure, and the muon rate changes accordingly. The solar diurnal component of the muon rate variation, when modulated by a seasonally varying signal, gives rise to spurious sidereal variation. In the celestial coordinate analysis below, we subtract this spurious variation from the observed signal using the method of Farley and Storey [2]. A detailed discussion of the muon rate variation due to atmospheric temperature variation and the method used to subtract the spurious sidereal variation from the observed variation is described in [9].

3. Celestial Coordinate Analysis

The cosmic ray anisotropy in the celestial sphere was plotted in one and two dimensions. In one dimension, a histogram of the right ascension of the muon arrival direction was made (with exposure equalization applied, as described in Sec. 2). In two dimensions, track-type maps are made in 10° slices of declination. Spurious sidereal variation of atmospheric origin described in Sec. 2 was subtracted from both the right ascension plot and the sky map. The spurious variation has little effect on the best fit value of the parameters describing the anisotropy, but it significantly increases the uncertainty.

The plot of the right ascension of cosmic rays before subtracting the spurious sidereal anisotropy from atmospheric effects is shown as data points in Fig. 1. The solid curve is the best fit of the first two harmonics to the data, while the dashed curve (almost overlapping the solid one) is the sidereal variation after correcting for the atmospheric effect. The solid curve is parameterized as follows:

$$F(x) = A_1 \cdot \cos\left[\frac{\pi}{180} \cdot (x - \phi_1)\right] + A_2 \cdot \cos\left[\frac{2\pi}{180} \cdot (x - \phi_2)\right] \tag{1}$$

The best fit parameter values after subtracting a small contribution from the spurious sidereal variation from the atmosphere are as follows: $A_1 = (6.6 \pm 1.0 \pm 0.6) \times 10^{-4}$, $\phi_1 = 33^\circ \pm 8^\circ \pm 5^\circ$, $A_2 = (4.1 \pm 1.0) \times 10^{-4}$, and $\phi_2 = 106^\circ \pm 7^\circ$. The amplitude and phase of the first harmonic has two errors, the first statistical, and the second systematic error introduced when subtracting the spurious atmospheric variation. The second harmonic errors are statistical only, since the spurious atmospheric variation is assumed to vary as a first harmonic function.

The anisotropy map in the celestial sphere is obtained by making track-type plots in 10° strips of declination, giving $10^\circ \times 10^\circ$ pixels. The result is shown in Fig. 2 (smoothing applied). A clustering algorithm [9] indicates an excess region toward the constellation Taurus $(\alpha_T, \delta_T) = (75^\circ \pm 7^\circ, -5^\circ \pm 9^\circ)$ and a deficit region toward Virgo $(\alpha_V, \delta_V) = (205^\circ \pm 7^\circ, 5^\circ \pm 10^\circ)$. The half opening angle of the "Taurus" region is $39^\circ \pm 7^\circ$ with a

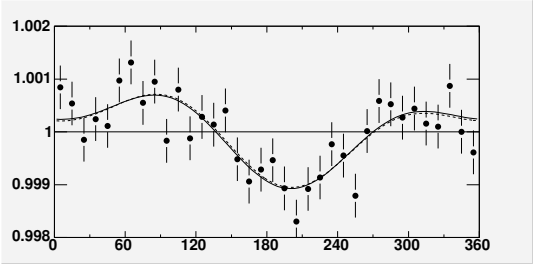

Figure 1. Plot of right ascension of muon arrival direction. The solid curve is the best fit of the first two harmonic functions. The dashed curve (almost overlapping the solid curve) is the first two harmonics after subtracting the spurious sidereal anisotropy of atmospheric origin.

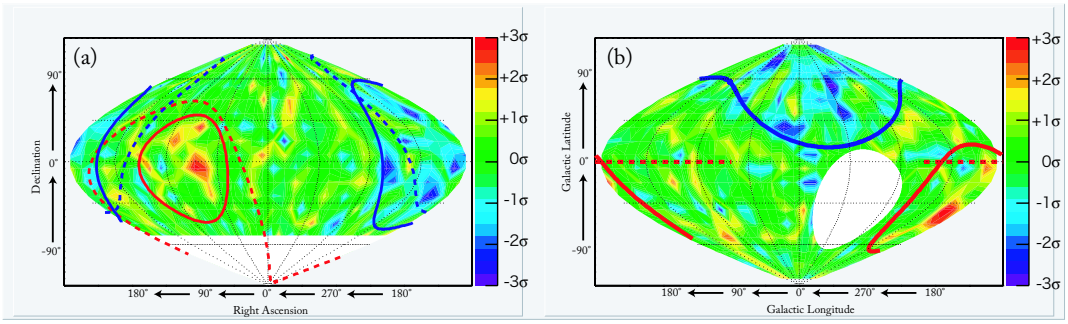

Figure 2. Sky map of the anisotropy in equatorial (a) and galactic (b) coordinates. The sky is divided into $10^\circ \times 10^\circ$ cells (Gauraud smoothing applied). Declinations less than -53.58° (white region) always lie below the horizon and are thus invisible to the detector. Each cell shows the standard deviation of the variation from isotropy. The solid red (blue) curve in (a) shows excess (deficit) cone obtained using a clustering algorithm applied to the data, while the dashed red (blue) curve shows the excess (deficity) cone from the NFJ model [4], which is described in Section 4. The dashed line in (b) indicates the direction of the Orion arm.

relative rate $(0.104 \pm 0.020)\%$ above isotropy, while the size of the "Virgo" region is $54^\circ \pm 7^\circ$ with a relative rate of $(0.094 \pm 0.014)\%$ below isotropy.

4. Discussion

One mechanism for producing cosmic ray anisotropy is by a gradient in the cosmic ray density. Although this is not well known, symmetry about the Galactic equator suggests that there is a density gradient component toward the Galactic south pole because the solar system is located about 20 pc to the north of the Galactic equator. Also, a component toward the Orion arm is expected because the solar system exists at the inner edge of the arm, in which supernova remnants tend to occur. Our observation supports this simple mechanism of cosmic ray anisotropy. The deficit region shown in Fig. 2 (b) covers a large part of the Galactic northern hemisphere. The region reaches furthest south roughly in the direction of the Galactic center, and recedes to far northern latitudes toward the Orion arm. This recession is consistent with the expectation that the cosmic

ray density is elevated toward the Orion arm, i.e. the excess flux from the Orion arm is presumably canceling out the deficit flux from the Galactic north.

Another mechanism for the anisotropy is given by the proponents of the so-called NFJ model [4]. In this model, the cosmic ray anisotropy observed in various cosmic ray experiments is explained by two conical zones in the celestial sphere, one from which excess flux is observed, and the other with deficit flux. The excess region, referred to as "Tail-In", is a cone centered in the direction $(\alpha_T, \delta_T) = (90^\circ, -24^\circ)$ with half opening angle $\chi_T \approx 68^\circ$, while the deficit region is centered at $(\alpha_G, \delta_G) = (180^\circ, 20^\circ)$ with half opening angle $\chi_G \approx 57^\circ$. These cones are indicated by dashed curves in Fig. 2. Our excess and deficit regions show fair agreement with the NFJ regions.

5. Conclusion

An anisotropy map of cosmic rays of nominal energy of 10 TeV was made from 1662 days of observation. The right ascension projection of this map has a first harmonic amplitude and phase of $(6.64 \pm 0.98\ \text{(stat.)} \pm 0.55\ \text{(syst.)}) \times 10^{-4}$ and $(33.2^\circ \pm 8.2^\circ\ \text{(stat.)} \pm 5.1^\circ\ \text{(syst.)})^\circ$. The sky map indicates a region with $(0.104 \pm 0.020)\%$ excess flux in the constellation of Taurus, while a region with $(0.094 \pm 0.014)\%$ deficit flux is observed in the constellation of Virgo. The excess region is centered at $(\alpha_T, \delta_T) = (75^\circ \pm 7^\circ, -5^\circ \pm 9^\circ)$ with a half opening angle of $39^\circ \pm 7^\circ$, while the corresponding values for the deficit region are $(\alpha_V, \delta_V) = (205^\circ \pm 7^\circ, 5^\circ \pm 10^\circ)$ and half opening angle $= 54^\circ \pm 7^\circ$. These regions are in good agreement with those of the NFJ model. The shape of the deficit region may be related to the cosmic ray density gradient in the neighborhood of the solar system.

6. Acknowledgements

We gratefully acknowledge the cooperation of the Kamioka Mining and Smelting Company. The Super-Kamiokande experiment has been built and operated from funding by the Japanese Ministry of Education, Culture, Sports, Science, and Technology, the United States Department of Energy, and the U.S. National Science Foundation. Some of us have been supported by funds from the Korean Research Foundation (BK21) and Korea Science and Engineering Foundation, the Polish Committee for Scientific Research (grant 1P03B08227), Japan Society for the Promotion of Science, and Research Corporation's Cottrell College Science Award.

References

[1] A. H. Compton and I. A. Getting, Phys. Rev. **47**, 817 (1935).
[2] F. J. M. Farley and J. R. Storey, Proc. Phys. Soc. A **67**, 996 (1954).
[3] K. Nagashima et al., Nuovo Cimento C **12**, 695 (1989).
[4] K. Nagashima, K. Fujimoto, and R. M. Jacklyn, J. Geophys. Res. No. A8 **103**, 17429 (1998).
[5] G. G. McGrath, Ph. D. thesis, University of Hawaii, Manoa (1993).
[6] K. Murakami et al., Nuovo Cimento C **2**, 635 (1979).
[7] S. Fukuda et al., Nucl. Instr. Meth. A **501**, 418 (2003).
[8] H. Ishino, Ph. D. thesis, University of Tokyo (1999).
[9] G. Guillian et al., "Observation of the Anisotropy of 10 TeV Primary Cosmic Ray Nuclei Flux with the Super-Kamiokande-I Detector". Draft in prepration.